

# Accelerated start-up of moving bed biofilm reactor by using a novel suspended carrier with porous surface

Xin Chen · Lingjun Kong · Xingyu Wang ·  
Shuanghong Tian · Ya Xiong

Received: 17 February 2014 / Accepted: 30 July 2014 / Published online: 9 August 2014  
© Springer-Verlag Berlin Heidelberg 2014

**Abstract** A novel suspended carrier with porous surface was firstly prepared by coating a sponge on the inside and outside of a hard polyethylene ring. Herein the effects of the sponge thickness (0, 2, 4, 6 mm) and pore size (17, 45, 85 pores per inch, ppi) on the performance of the start-up stage in moving bed biofilm reactor (MBBR) were investigated. The results indicated that the home-made carrier with the sponge thickness of 4 mm and the pore size of 45 ppi, defined as SC4-45, showed the best performance, which obtained high biomass concentration of 2,136.6 mg/L, oxygen uptake rate for COD of 150.1 mg O<sub>2</sub>/h and oxygen uptake rate for NH<sub>4</sub><sup>+</sup>-N of 17.4 mg O<sub>2</sub>/h. The DGGE profiles of the biofilms obtained in SC4-45 and a commercial carrier showed a similar community as the Dice similarity coefficients between two samples was 0.72. Furthermore, 16S rRNA gene sequence analysis reveals dominance of *Sphaerotilus* sp. and *Aeromonas* sp. in the community of both samples. Moreover, for the MBBR based on SC4-45, COD and NH<sub>4</sub><sup>+</sup>-N removal rates reached 99.5 ± 1.1 and 93.6 ± 2.3 % at the end of the start-up stage, much higher than those of the commercial carrier,

74.9 ± 2.7 and 40.0 ± 1.8 %, respectively. These indicated the novel carrier obtained a quick start-up.

**Keywords** Moving bed biofilm reactor · Suspended carrier · Start-up · Sponge · Bacterial activity

## Introduction

Up to now, there are many different biofilm treatment plants in use, such as trickling filters [1], submerged membrane bioreactors [2], fixed media submerged biofilters [3, 4], granular media biofilters [5], fluidized bed reactors [6, 7] and moving bed bioreactors (MBBR) [8, 9]. Among those systems, MBBR has developed as a highly effective and reliable biological technology for carbon and nitrogen removal by combing the advantages of the conventional activated sludge process and the fluidized bed reactor [10]. By using carriers that can move freely throughout the entire volume of the reactor, the MBBR system has many advantages such as simple construction, low space requirement [11], low sludge production [12, 13], high biomass concentration and long sludge residence time (SRT) [14]. Ammonia removal from polluted raw water was recently successfully achieved in MBBRs, since suspended carriers can provide an attachable surface for slow-growing microorganisms such as nitrifying bacteria [15] and anammox bacteria [16–18].

In the MBBR system, carriers, on which the biomass attach and live, are the key materials determining the efficiency and performance of treating wastewater [19, 20]. Many researchers have worked with different carriers like polyurethane cubes (LINPOR and CAPTOR types) [21], polystyrene beads [22], polyethylene cylinders (Kaldnes types) [12, 23], activated carbon particles [24] and carriers

X. Chen · L. Kong · X. Wang · S. Tian (✉) · Y. Xiong (✉)  
School of Environmental Science and Engineering, Sun Yat-sen  
University, Guangzhou 510275, People's Republic of China  
e-mail: t-sh-h@163.com

Y. Xiong  
e-mail: cesxya@mail.sysu.edu.cn

X. Chen  
e-mail: chenxin8@mail2.sysu.edu.cn

X. Chen · L. Kong · X. Wang · S. Tian · Y. Xiong  
Guangdong Provincial Key Laboratory of Environmental  
Pollution Control and Remediation Technology,  
Guangzhou 510275, People's Republic of China

made from polymers like polyhydroxybutyrate or polycaprolactone [25]. The carriers are mainly grouped as two categories: non-porous carriers with smooth surface such as Kaldnes types and porous carriers such as LINPOR and CAPTOR types. The non-porous carriers are usually made from polyethylene or polypropylene and have high durability and stability, which are widely used in the wastewater treatment plants and in the lab. However, they have some drawbacks of low specific surface area (about  $500 \text{ m}^2/\text{m}^3$ ) [26], leading to slow start-up and easy detachment of biofilm due to the smooth surface. On the contrary, the porous carriers can escape from those drawbacks due to the excellent porous structure, which can not only trap and intercept the biomass efficiently and thereof shorten the start-up period, but also promote biofilm accumulation by providing a large surface area ( $5,000\text{--}35,000 \text{ m}^2/\text{m}^3$  for LINPOR) [27] and protect the biofilm from fluid shearing and collision by providing sheltered anchoring points. However, the porous carriers suffer a lot from the low mass transfer efficiency. Kjetil Rasmussen et al. [28] pointed out that in the membrane system, there was a minor distinction in local mass transfer resistance in thin biofilm ( $70 \mu\text{m}$  or less). The local mass transfer coefficients in biofilm clusters  $350 \mu\text{m}$  thick and more decreased gradually, approaching zero near the substratum. So, it is difficult for the mass to transfer deep inside the porous carrier, which makes most of the surface area useless. Therefore, it is very significant to develop new carriers that can overcome the low mass transfer efficiency of the current porous carriers.

In this study, a novel suspended carrier with porous surface was prepared by coating a porous layer on the inside and outside of a hard polyethylene ring. For such a novel structure, the first advantage is that the porous layer can supply a large surface area for the attachment and growth of the bacteria and thereof accelerate start-up of MBBR. The second advantage is that the mass transfer efficiency could be enhanced. When the moving carriers come into collision, the elastic porous surfaces are compressed and the purified water is extruded out. After the completion of collision, the porous surface would stretch to the normal state and absorb wastewater immediately. Thus, the high mass transfer efficiency could be obtained in spite of thick biofilm.

Herein, the study is mainly focused on the relationship of the carrier structure, biofilm characteristics and the wastewater treatment efficiency, containing three aspects: (I) effect of the thickness of porous layer and pore size on the attached biomass concentration and nutrient removal; (II) bacterial activity and microbial community of biofilm on the carriers, (III) compare the novel carrier and the commercial carrier on the aspect of COD,  $\text{NH}_4^+\text{-N}$ , TN removal efficiency during the start-up period. The objective

of this study is to investigate the possibility of application of the novel suspended carriers in MBBR to treat wastewater with quick start-up and high performance.

## Materials and methods

### Materials

Analytical grade of potassium dichromate, iron ammonium sulfate, potassium sodium tartrate, ammonium chloride, sulfuric acid, silver sulfate, mercuric iodide, potassium iodide were purchased from Tianjin Fucheng Chemical Reagent Co. Ltd., China. Guarantee reagents of sodium nitrite and nitrate of potassium were purchased from Tianjin Chemical Reagent Co. Ltd., China. The biofilm carrier named as BioM<sup>®</sup> was commercially supplied by Dalian Yudu Environmental Materials Co. Ltd., China.

### Synthetic wastewater

The experiments were conducted using a synthetic wastewater to avoid any fluctuation in the feed concentration. The synthetic feed water was supplied with  $\text{CH}_3\text{COONa}$ ,  $\text{NH}_4\text{Cl}$ ,  $\text{KH}_2\text{PO}_4$  at a mass ratio of  $\text{COD:N:P} = 100:10:1$  and the influent COD concentration of about  $250 \text{ mg/L}$  and  $\text{NH}_4^+\text{-N}$  concentration of about  $25 \text{ mg/L}$ . The influent COD concentration and  $\text{NH}_4^+\text{-N}$  concentration were actual measured values. Mineral salt was prepared using stock solution ( $\text{EDTA}$ ,  $5 \text{ g/L}$ ;  $\text{ZnSO}_4 \cdot 7\text{H}_2\text{O}$ ,  $0.43 \text{ g/L}$ ;  $\text{CoCl}_2 \cdot 6\text{H}_2\text{O}$ ,  $0.29 \text{ g/L}$ ;  $\text{MnSO}_4$ ,  $0.85 \text{ g/L}$ ;  $\text{CuSO}_4$ ,  $0.16 \text{ g/L}$ ;  $\text{NiCl}_2 \cdot 6\text{H}_2\text{O}$ ,  $0.19 \text{ g/L}$ ;  $\text{H}_3\text{BO}_4$ ,  $0.014 \text{ g/L}$ ;  $\text{FeCl}_3$ ,  $3.4 \text{ g/L}$ ) which were mixed with tap water at a volumetric ratio of 0.001:1. Sodium hydrogen carbonate was used as a buffer to adjust the mixed liquor pH to about 7.5–8.0. The temperature of the mixed liquor was controlled at  $25.0 \text{ }^\circ\text{C}$  with an air conditioner.

### Preparation of suspended carrier with porous surface

The suspended carriers with porous surface were made of sponges and polyethylene rings. A polyethylene tube (Ginde Corp. Ltd.) with an outside diameter of  $20 \text{ mm}$ , a wall thickness of  $2 \text{ mm}$  and a density of  $0.91 \text{ g/cm}^3$  was cut into rings with length of  $10 \text{ mm}$ . And the polyurethane sponges (Shanghai Yinke Co. Ltd.) with different pore size ( $17, 45, 85 \text{ ppi}$ ) served sliced into different thickness ( $2, 4, 6 \text{ mm}$ ) were glued to the inside and outside of the polyethylene rings; ppi means pores per inch, which represented the pore size of a sponge.

The home-made suspended carriers were named as  $\text{SC}_{x-y}$ , and  $x$  represented the thickness of porous surface while  $y$  means the pore size of the sponge. When the pore

size of the sponge was fixed at 45 ppi (45 pores per inch), the suspended carrier with the porous surface of 0, 2, 4, 6 mm in thickness was named as SC0, SC2-45, SC4-45, SC6-45. When the thickness of the porous surface was fixed at 4 mm, the carrier with sponge pore size of 17, 45 and 85 ppi was labeled as SC4-17, SC4-45 and SC4-85, respectively. The commercial biofilm carrier named as BioM<sup>®</sup> was used for comparison. The commercial carrier is a cylinder with diameter of 20 mm, a height of 20 mm and density of 0.96–0.98 g/cm<sup>3</sup>. The carrier had crisscross sheets inside to divide the cylinder into four sectors.

### Reactor operation

Experiments were conducted in five identical apparatus. The effective volume of each bioreactor was 1.9 L. Each kind of carriers with the same working volume (filling ratio, 30 %) was put into each reactor, respectively. The air was introduced through a distributor on the bottom of the reactor. The synthetic water was fed continuously. The hydraulic retention time (HRT) was set at 6 h. The aeration intensity for all the five reactors was 25 L/h. The DO of reactors was maintained between 6.2 and 7.1 mg/L with the average value at about 6.5 mg/L during the total trial period. Complete sludge retention time ( $SRT = \infty$ ) was applied in MBBR. The reactors were operated for 7 days without sludge discharge, when completing the start-up and optimization.

Each reactor was seeded with 500 mL of a mixed culture at the concentration of 6,500 mg/L taken from the municipal wastewater plant, and then the culture was incubated for approximately 24 h to encourage microbial growth and adhesion on the carriers. Then the water including the suspended cultures was removed from the reactors and the system with suspended carrier was continuously fed with the fresh synthetic water.

### Analytic methods

#### *Water quality analysis*

Water quality analysis was conducted following the standard methods [29]. COD was analyzed by the oxidation method using potassium dichromate.  $NH_4^+$ -N,  $NO_2^-$ -N and  $NO_3^-$ -N concentrations were determined by the colorimetric methods using a spectrometer (UV2450, Shimadzu, Japan). DO and pH in the reactor were measured by a DO (YSI 550A, USA) and pH (Leici PHS-25, China) meter, respectively. TN was calculated by the sum of  $NH_4^+$ -N,  $NO_2^-$ -N and  $NO_3^-$ -N since  $NH_4Cl$  was the only nitrogen source in the feed wastewater. Mixed liquor suspended solids (MLSS) was analyzed by gravimetric method. For measuring MLSS, three samples were taken

each time and the average values were then calculated. Homogeneity of group variances were checked by using *F* test, and the effects of porous layer thickness and pore size on COD removal efficiency were determined by multivariate analysis of variance (MANOVA) test, at a significance level of  $p = 0.05$ . All the statistical analyses were performed by SAS<sup>®</sup> 9.4 software (SAS Institute Inc.).

#### *Biofilm analysis*

Photomicrograph was made in order to observe the biofilm features and structure in the experiments.

Attached biomass concentration was determined by drying the mixed liquor sample at 105 °C for 24 h. The procedure in detail was as follows: quantity of carriers were taken out from the bioreactor and dried to a constant weight in an oven at 105 °C for 2 h. The dry weight including biofilm and carrier was labeled as  $W_1$ . The dry carriers were kept stirring in 0.1 mol/L of hydrochloride solution for 2 h at 80 °C and then treated in an ultrasonic for 1 h, followed by washing with water several times until all the biofilm was removed from the carrier. Finally, the carriers were dried to a constant weight in an oven at 105 °C for 2 h. The dry weight of the net carriers was labeled as  $W_2$ . Thus the weight of the biofilm was obtained by equation of  $W_1 - W_2$ . Attached biomass concentration in the bioreactor can be calculated based on the ratio of carriers taken out of the bioreactor and the volume of the bioreactor.

Microbial activity was quantified with a respirometric technique by the following procedure [30]: briefly, an 800-mL completely sealed glass vessel with a port at the top for the insertion of a DO probe was employed for respirometry. The DO probe was connected through a RS-232 port to a personal computer, which was used for storing and monitoring all data transmitted by the probe. After 7-day start-up operation, carriers with biofilm were washed tenderly and added to the vessel filled up with 800 mL of tap water. The suspension was aerated with air for approximately 1 min to obtain dissolved oxygen (DO) higher than 6 mg/L. Then aeration was ceased and substrate aliquots (no substrate for endogenous respiration, 25 mg/L of  $NH_4^+$ -N for the oxygen uptake of  $NH_4^+$ -N oxidation and 250 mg/L of the oxygen uptake of COD oxidation) were added. A decrease in the DO level due to substrate oxidation was measured by a DO probe and continuously recorded by a personal computer interfaced to a DO monitor. A running linear regression was performed. Then the oxygen uptake rate in the reactor, noted as  $OUR_{ER}$  (oxygen uptake for endogenous respiration),  $OUR_{NH_4}$  (oxygen uptake for  $NH_4^+$ -N oxidation),  $OUR_{COD}$  (oxygen uptake for COD oxidation) correspondingly, was calculated according to the slope

value and the ratio of carriers taken out for measurement and the total carriers in the reactor. The specific oxygen uptake rate, noted as  $SOUR_{ER}$  (specific oxygen uptake for endogenous respiration),  $SOUR_{NH_4}$  (specific oxygen uptake for  $NH_4^+$ -N oxidation),  $SOUR_{COD}$  (specific oxygen uptake for COD oxidation) correspondingly, was calculated by the OURs and the amount of attached biomass.

Substrate degradation rate (SDR) is another indicator for bacterial activity [31]. After 7-day start-up stage, the mix liquor in the reactor was drained and replaced by fresh synthetic wastewater. Then in the following 10 h, COD and  $NH_4^+$ -N concentrations were measured every 2 h.

#### Microbial community analysis

Carriers were taken from the reactors after the 7 days of operation. The biofilm was scraped off the carriers after being homogenized by ultrasonic for 10 min. The carriers were subsequently washed by deionized water for 3 times. The liquid and biofilm were centrifuged at 12,000g for 10 min at 4 °C to collect cells. DNA was extracted from the biofilm samples by using the BIOMEGA Soli DNA extraction kit according to the manufacturer's protocol. Amplification of the 16S rRNA gen was performed in the extracted DNA samples with the primers 341F-GC and 518R for bacterial community analysis. The thermal profile for amplification was: 4 min at 94 °C, 30 cycles of 30 s at 94 °C, 30 s at 56 °C and 60 s at 72 °C, and a final 10 min at 72 °C. PCR products were spotted in 1 % agarose gel and electrophoresed at 100 V for 25 min. Then the agarose gel was visualized with fluorescent transilluminator to assess the purity and concentration of DNA. 40 % acrylamide gel, in TAE buffer (50×), with a linear denaturing gradient (urea, formamide, TEMED, and 10 % APS) from 35 to 65 % was using to assay the PCR products. Electrophoreses were performed at 80 V in 1× TAE buffer at a constant temperature of 60 °C for 15 h. Bands were stained and visualized with fluorescent transilluminator. Some dominant bands were manually excised from the gel and used as a template in a re-amplification, using primers 341F and 518R. The same amplification protocol was applied. PCR products were purified and sequenced at Beijing Genomics Institute (BGI) Co. Ltd., China. The sequences obtained were compared with 16S rRNA gene sequences in the NCBI database.

All the experiments and analyses were performed in April 2013, in the Laboratory of School of Environmental Science and Engineering, Sun Yat-Sen University, Guangzhou, P. R. China and in the Guangdong Provincial Key Laboratory of Environmental Pollution Control and Remediation Technology, Guangzhou, P. R. China.

## Results and discussion

### Optimization of the novel suspended carrier

#### *Effect of porous layer thickness on biofilm characteristics and wastewater treatment efficiency*

Suspended carriers with different thickness of porous layer (0, 2, 4 and 6 mm, with the same pore size of 45 ppi, corresponding to SC0, SC2-45, SC4-45, SC6-45, respectively) were applied in MBBR and operated for 7 days at the HRT of 6 h, to check the dependence of porous layer thickness on biofilm amount. The transverse profile along the porous layers on the seventh day is shown in Fig. 1. It can be seen from the appearance that the porous layers are filled by microorganisms. It further proved that the whole porous layers for three types of carriers are occupied by biomass.

In a biological treatment process, attached biomass concentration is an important factor to ensure the biological treatment ability. The attached biomass concentration on suspended carriers with different porous layer thickness versus time is shown in Fig. 2. Since the seed sludge can penetrate the porous layer and adsorb on it easily, the attached biomass concentration on SC2-45, SC4-45, SC6-45 on day 1 has already reached 202.1, 541.7 and 884.4 mg/L, respectively. It is obvious that the attached biomass concentration increased with the porous layer thickness and the start-up time. Moreover, microorganisms step into the period of rapid growth on day 3 and the attached biomass concentration increased sharply. After day 5, the growth rate decreased and the attached biomass concentration on different suspended carriers are almost steady on day 7. These facts proved that the porous structure (SC2-45, SC4-45, SC6-45) favored the attachment and growth of biofilm on it and the smooth surface of polypropylene (SC0) showed the opposite effect. That is because the thicker porous layer can trap and intercept more biomass efficiently and the reticulate structure can promote biofilm accumulation by providing a large surface area [32]. The intensification in attached biomass concentration revealed the potential capability of MBBR be operated at higher organic loading and the equipment volume can thus be reduced. It is worth mentioning that attached biomass concentration on SC4-45 is only slightly lower than that on SC6-45, which means that the density of biofilm on SC6-45 is much lower than that on SC4-45. On one hand, low density of the biofilm indicates the bacteria in the deep biofilm does not have access to enough food for their growth. On the other hand, low density favors mass transfer and can supply substrate for the growth of the bacteria to the depth of 6 mm on SC6-45. In contrast, biofilm on SC2-45 is always lesser than those on SC4-45

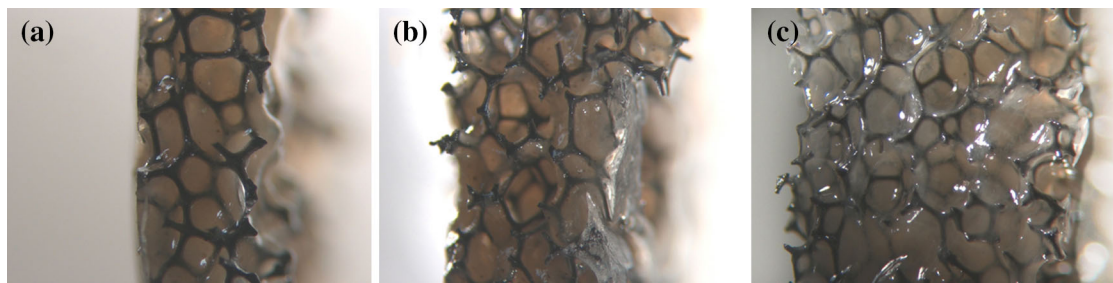


**Fig. 1** Microscope profiles of the biofilm on different carriers (a SC2-45, b SC4-45, c SC6-45, magnified 19 times)

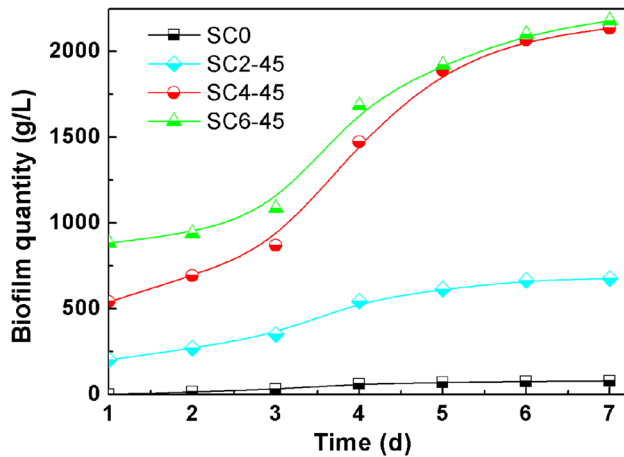


**Fig. 2** Attached biomass concentration changes against time in the start-up stage

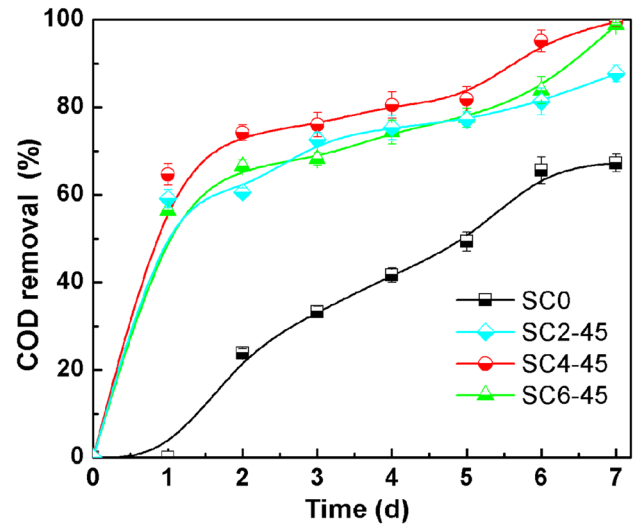


**Fig. 3** COD removal efficiencies against the time in start-up stage

and SC6-45 and increased slowly possibly because the porous layer is not thick enough to protect the biofilm from fluid shearing and the biofilm renewed very often.

According to the above discussion, the attached biomass concentration, an important factor to ensure the biological treatment ability, depends on the porous layer greatly. Moreover, COD removal efficiency is an important parameter in biological processes, which defines organic matter removal in unit volume and time. Therefore, the dependence of porous layer thickness on COD removal efficiency was investigated to determine the optimal porous layer thickness.

The various porous layer thicknesses contributed largely to a significant difference in COD removal efficiency, as the MANOVA test showed ( $p < 0.001$ ). As shown in Fig. 3, COD removal efficiency of home-made suspended carriers increased sharply on day 1. Afterwards, they progressively changed with the time. The effluent COD of the home-made suspended carriers with porous layer SC2-45, SC4-45, SC6-45 exceeded 60 % of COD removal efficiency on day 2, especially the value is  $74.2 \pm 1.8$  % for SC4-45, much higher than that for SC0. On day 7, above 80 % of COD removal efficiency was obtained for SC2-45,

SC4-45 and SC6-45 and almost 100 % for SC4-45 and SC6-45. That can be explained by the formation of biofilm and the characteristic of the home-made suspended carriers. Usually the formation of biofilms contains four steps [33]: firstly, some suspended cells are transported from liquid to a carrier surface by physical movement. Secondly, initial attractive forces, which are various physical forces and chemical forces, retain some cells on the carrier surface, and further promote stable multicellular contacts. Thirdly, microbial force makes the attached cells mature. Lastly, the biofilms would be finally shaped by hydrodynamic shear force to form a certain structured community. The outer shape and size of biofilms are holistically determined by the interactive strength/pattern between aggregates and hydrodynamic shear force, microbial species and substrate loading rate and so on. The porous structure on the surface of the home-made carrier could not only trap and intercept the biomass efficiently to shorten the start-up period, but also promote biofilm accumulation by providing a large surface area for attachment and protect the biofilm from fluid shearing and collision by providing sheltered anchoring points [27]. This special structure

promotes the formation of biofilms and the stable biofilm could be obtained very quickly. SC4-45 exhibited the highest COD removal efficiency, which is in agreement with the fact that SC4-45 has very high attached biomass concentration. Hence, the optimal porous layer thickness was determined as 4 mm.

#### *Effect of pore size on biofilm characteristics and wastewater treatment efficiency*

The attached biomass concentration on carriers with three different pore sizes (17, 45, 85 ppi) and the same thickness of sponge layer (4 mm), namely SC4-17, SC4-45, SC4-85, was measured after 7 days of operation. The thickness of biofilm on SC4-17, SC4-45, SC4-85 all equals to the thickness of porous layer of 4 mm, while the attached biomass concentration of SC0, SC4-17, SC4-45 and SC4-85 in each reactors are 79.7, 1,860.5, 2,136.6 and 1,746.9 mg/L, respectively. The biomass concentration follows the order of SC4-45 > SC4-17 > SC4-85. As is discussed previously, porous structure can promote biofilm accumulation by providing a large surface area for attachment and protect the biofilm from being washed out by fluid shearing and collision. When the pore size increased, the surface area and the sheltered anchoring points for bacterial decreased. Moreover, the biofilm is not homogenous, consisting of cell clusters and voids. In cell clusters molecular diffusion is the predominant transport mechanism while in voids both diffusion and convection are possible [34]. The mass transfer efficiency can be greatly improved by convection. Thus if the pore size is too small, less voids will be available in the biofilm and result in worse substrate and oxygen transport to the inner regions. That would be the possible reason that SC4-45

with middle pore size possessed the highest attached biomass concentration.

During the 7 days after seeding sludge, COD removal efficiency increased with the time, as shown in Fig. 4. The p value from MANOVA test was less than 0.001, which indicated there was a significant difference in COD removal efficiency among carriers with different pore size. It is obvious that the COD removal efficiencies of all the home-made suspended carriers with porous layer (SC4-17, SC4-45, SC4-85) are all superior to that of SC0. Moreover, SC4-45 exhibited the highest COD removal efficiency, which is in agreement with the fact SC4-45 has the highest attached biomass concentration. Hence, the optimal pore size was determined as 45 ppi.

#### Biofilm performance

The performance of bacterial activity on novel suspended carrier SC4-45 was investigated by comparing oxygen uptake rate (OUR) and substrate degradation rate (SDR) with SC0 and commercial carrier BioM<sup>®</sup>. Microbial community on SC4-45 and BioM<sup>®</sup> was analyzed through molecular biological technology.

#### *Oxygen uptake rate (OUR)*

Oxygen uptake rate (OUR), as a direct measurement of biokinetic rates, plays a crucial role in MBBR since oxygen is required to remove both nitrogen and carbon. In a biofilm process, several parameters such as attached biomass concentration, wastewater type, mixing characteristics, the availability of substrates and nutrients and the presence of toxins, can influence oxygen uptake rate. In this study, respiration test was conducted using the carriers with biofilms taken from the bioreactors on the seventh day of the start-up stage. The typical plot of the oxygen concentration during intermittent aeration for biofilm attached on SC4-45 is shown in Fig. 5. Three zones are for the oxygen uptake of endogenous respiration (OUR<sub>ER</sub>) without addition any substrate, the oxygen uptake for NH<sub>4</sub><sup>+</sup>-N oxidation (OUR<sub>NH4</sub>) with the addition of only ammonium and the oxygen uptake for COD oxidation (OUR<sub>COD</sub>) with the addition of only acetate, respectively. It is obvious that the relationship between the decrease in oxygen concentration and the time is almost linear. The oxygen uptake rate is determined by calculations of the slope of the curve according to Eq. 1. The specific oxygen uptake rate is obtained if the oxygen uptake rate is related to the attached biomass concentration attaching on the carriers according to Eq. 2, employed by Awong et al. [35]. All the curves of OUR measurement for biofilm attached on different carriers are similar to the curves shown in Fig. 5. Hence, only data are given in Table 1 for comparison.

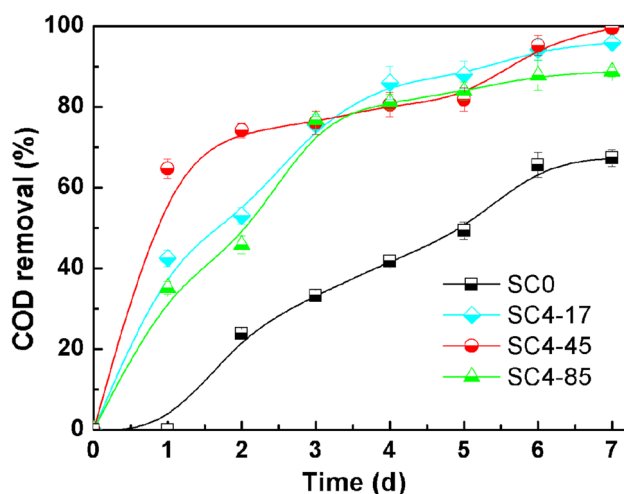
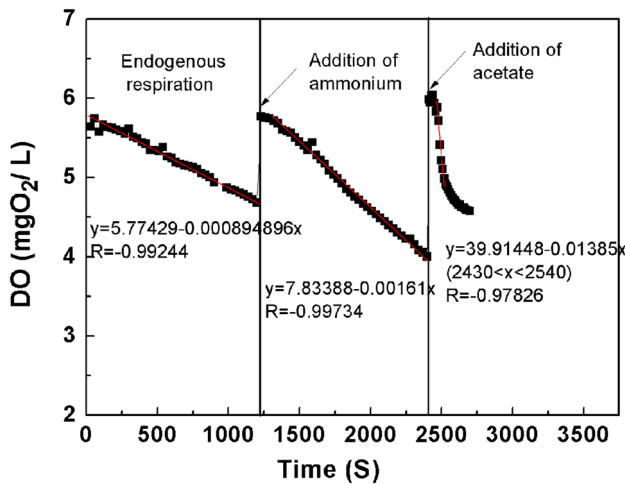


Fig. 4 COD removal efficiencies against time in the start-up stage



**Fig. 5** Typical plot of the oxygen concentration during intermittent aeration for biofilm attached on SC4-45

**Table 1** Characteristics of biofilm on carriers with different sponge thickness

| Carrier type  | SC0   | SC4-45 | BioM® |
|---|-------|--------|-------|
| OUR <sub>ER</sub> , mg O <sub>2</sub> /h                      | 5.0   | 9.7    | 2.2   |
| OUR <sub>NH<sub>4</sub></sub> , mg O <sub>2</sub> /h          | 5.2   | 17.4   | 2.0   |
| OUR <sub>COD</sub> , mg O <sub>2</sub> /h                     | 16.1  | 150.1  | 19.2  |
| SOUR <sub>ER</sub> , mg O <sub>2</sub> /(gMLSS h)             | 33.0  | 2.4    | 22.6  |
| SOUR <sub>NH<sub>4</sub></sub> , mg O <sub>2</sub> /(gMLSS h) | 34.3  | 4.3    | 20.5  |
| SOUR <sub>COD</sub> , mg O <sub>2</sub> /(gMLSS h)            | 106.3 | 37.0   | 197.3 |

$$OUR = \frac{DO_0 - DO}{\Delta t} \times r = k_d \times 3,600 \times r \quad (1)$$

$$SOUR = \frac{OUR}{c \times V} \quad (2)$$

where  $k_d$  is the oxygen uptake rate of the measured biofilm and obtained from the slope of corresponding line,  $r$  is the quantity ratio of carriers in the whole reactor and carriers taken out for OUR measurement,  $c$  is the attached biomass concentration in the whole reactor,  $V$  is the volume of the bioreactor.  $OUR_{ER}$ ,  $OUR_{NH_4}$ ,  $OUR_{COD}$  is the oxygen uptake rate of endogenous respiration, only  $NH_4^+-N$  as substrate and only COD as substrate, respectively.

The endogenous respiration is often defined as the oxygen consumption of microorganisms in the absence of substrate, but many mechanisms and processes are included in the conception of endogenous respiration. SC4-45 showed the highest  $OUR_{ER}$  of 9.7 mg O<sub>2</sub>/h, at least twice as that of others. Moreover, the highest  $OUR_{NH_4}$  for SC4-45, 17.4 mg O<sub>2</sub>/h, indicates fast ammonia oxidation under constant and sufficient aeration. In contrast, the lowest  $OUR_{NH_4}$  occurred in the MBBRs based BioM®. This

showed that the total activity of nitrobacteria attached on SC4-45 was high and the MBBR based on SC4-45 should exhibit good wastewater treatment performance. Acetate is often used as reference substrate since it is a very easily degradable organic matter for heterotrophic bacteria. The  $OUR_{COD}$  in the MBBR based on SC4-45 was 150.1 mg O<sub>2</sub>/h, over seven times higher than that of BioM®. High  $OUR_{COD}$  may be indicative of complete oxidation (and storage metabolism).

The specific oxygen uptake rate can indicates the bacterial activity per gram of attached biomass.  $SOUR_{ER}$ ,  $SOUR_{NH_4}$ ,  $SOUR_{COD}$  decreased with increasing the thickness of the biofilm, indicating that the bacterial activity decreased. That can be explained by the fact that the mass transfer of substrates, nutrients and oxygen to the inner bacterial becomes more difficult when the biofilm becomes thicker and result in the decrease of the bacterial activity. OUR is determined by both the quantity of fixed biofilm and the mass transfer efficiency of oxygen and substrates. Therefore, the biofilm on SC4-45 showed the highest OUR due to the combination of bacterial activity and high attached biomass concentration. It implies that the MBBR using SC4-45 would probably show the best wastewater treatment performance.

The mixed liquor suspended solids (MLSS) at day 7 in MBBR is 16.7, 40.8, 14.9 mg/L, for SC0, SC4-45, BioM®, respectively, less than 20 % of the total amount of biomass concentration. Due to the low proportion of MLSS, high volume of settler was needless to lower land requirement of the wastewater treatment plant potentially.

*Substrate degradation rate (SDR)*

Substrate degradation rate is another parameter directly indicative of biofilm activity. After 7 days of acclimatization, the carriers were taken out from the reactors to conduct a batch experiment. The COD degradation rate in 10 h with an initial COD concentration of 250 mg/L was determined in a batch reactor, as shown in Fig. 6a. The COD removal efficiency SC4-45 and BioM® increased sharply during the first 2 h of the reaction period. After the beginning of the substrate injection, and the SDR for SC0, SC4-45 and BioM® was 71.7, 90.8, 82.0 mg COD/(L h), respectively. Afterwards, the COD removal efficiency increased slowly and almost kept steady at the level of approximately 80 %. It could be interpreted that the bacteria could be subjected to unlimited supply of food and oxygen at first, which encouraged the growth of biomass bacteria. As the biodegradation continued, the substrate was consumed gradually. The substrate became limiting and the bacteria came into starvation. Although substrate consumption rates can be correlated with physical characteristics, such as roughness and surface area, the actual

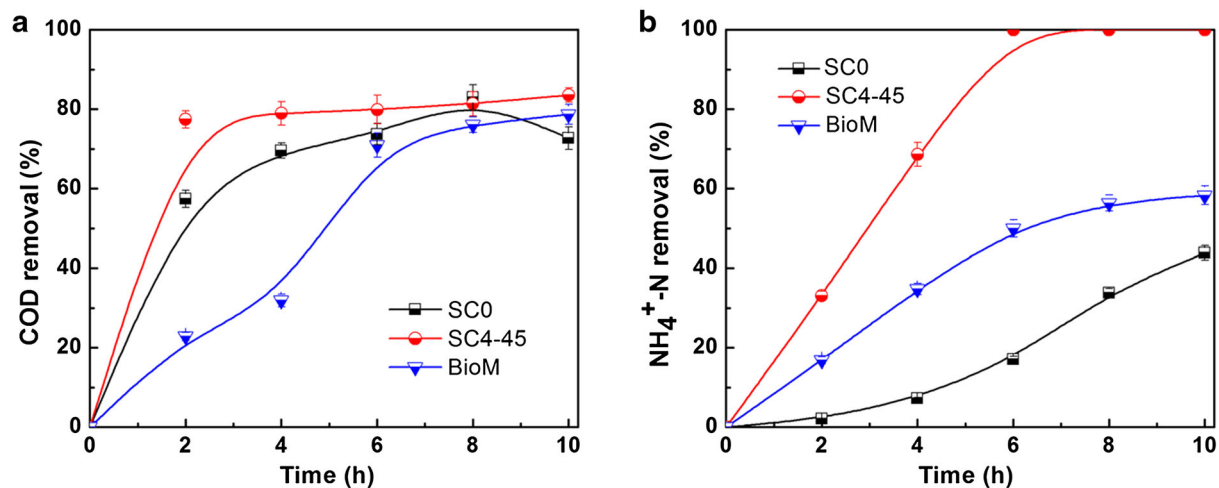


**Fig. 6** Substrate degradation rate (SDR) of SC4-45, SC0 and BioM<sup>®</sup> (a COD degradation rate, b NH<sub>4</sub><sup>+</sup>-N degradation rate)

difference among the carriers in terms of substrate consumption rates may be fundamentally caused by the accessibility of the carrier surface area to substrate and oxygen, which is usually considered to be the substance limiting for cell growth. It was recognized that even at the saturation level of oxygen and enough food in the water, it is likely that the inner surface of the biofilm on some of the carriers may be oxygen and substrate limited, and thus the differences in substrate consumption rate observed among the carriers in the experiments may be directly attributed to differences in oxygen and substrate availability at the inner layer of the biofilm. It was noticeable that SC4-45 already had the COD removal efficiency of 80 % in 2 h. This result is in accordance with the bacterial activity indicated by the  $SOUR_{COD}$  measurement.

The NH<sub>4</sub><sup>+</sup>-N degradation rate in 10 h with initial NH<sub>4</sub><sup>+</sup>-N concentration of 25 mg/L was also determined in a batch reactor, as shown in Fig. 6b. Unlike the COD degradation rate, The NH<sub>4</sub><sup>+</sup>-N removal efficiency with obvious difference follows the order of SC4-45 > BioM<sup>®</sup> > SC0. For SC4-45, NH<sub>4</sub><sup>+</sup>-N removal efficiency reached 100 % in 6 h, supporting that there are many active nitrifiers in the biofilm attached on SC4-45, which accords with results that SC4-45 showed the highest  $OUR_{NH_4-N}^+$  among all the carriers.

#### Microbial community of biofilm

DGGE fingerprints were obtained by analyzing the bacterial DNA extracted from biofilm samples of SC4-45 and BioM<sup>®</sup> (Fig. 7). Although differences in the bacterial activity of the biofilms were found, the DGGE profiles of the biofilms obtained in SC4-45 and BioM<sup>®</sup> showed similar microbial population structure as the Dice similarity coefficients between two samples was 0.72. Close relatives

of the excised bands were identified with cultured organisms in the NCBI nucleotide sequence database (Table 2). The sequence of these bands A3, A6, B3, B6 were 96 % similar to *Aeromonas* sp., which can degrade organic matter and transform nitrate into nitrite in the activated sludge system [36]. Bands A1, A9, A10, A11 of SC4-45 and B9, B10 were identified as close relatives of *Sphaerotilus* sp. and *Sphaerotilus natans*, which commonly causes a filamentous bulking in activated sludge and poor settling in CASS systems [37, 38]. Figure 7 and Table 2 indicated that *Sphaerotilus* sp. and *Aeromonas* sp. were the majority in the bacterial community of SC4-45 and BioM<sup>®</sup>. The gamma proteobacterium group (A7) is responsible for the nitrogen and phosphorus removal [39]. *Pseudomonas* sp. (A8) is involved in denitrification and nitrate reduction to nitrite [38]. In BioM<sup>®</sup>, bands B7 and B8 corresponded phylogenetically to *Flavobacterium* sp. (97 %) and *Acidovorax* sp. (98 %), respectively. It seems that the culture of SC4-45 was more plentiful than that of BioM<sup>®</sup>. One possible reason is that anoxic zones cause by the oxygen diffusion limitation along the biofilm-inward depth, would make abundant bacterial communities on SC4-45.

#### Comparison of SC4-45 and the commercial carrier in the start-up stage

Comparative researches were carried out among the reactors with different carriers, SC4-45, SC0 and BioM<sup>®</sup>. The removal efficiencies of COD and NH<sub>4</sub><sup>+</sup>-N, and the performance of nitrification/denitrification were investigated during the start-up stage. The MBBR reactors were operated with the influent COD of 250 mg/L, NH<sub>4</sub><sup>+</sup>-N of 25 mg/L and HRT of 6 h. The pH of synthetic wastewater varied from 7.5 to 8.0 during the whole experiment. The effluent pH of MBBR with SC4-45, SC0 and BioM<sup>®</sup> were



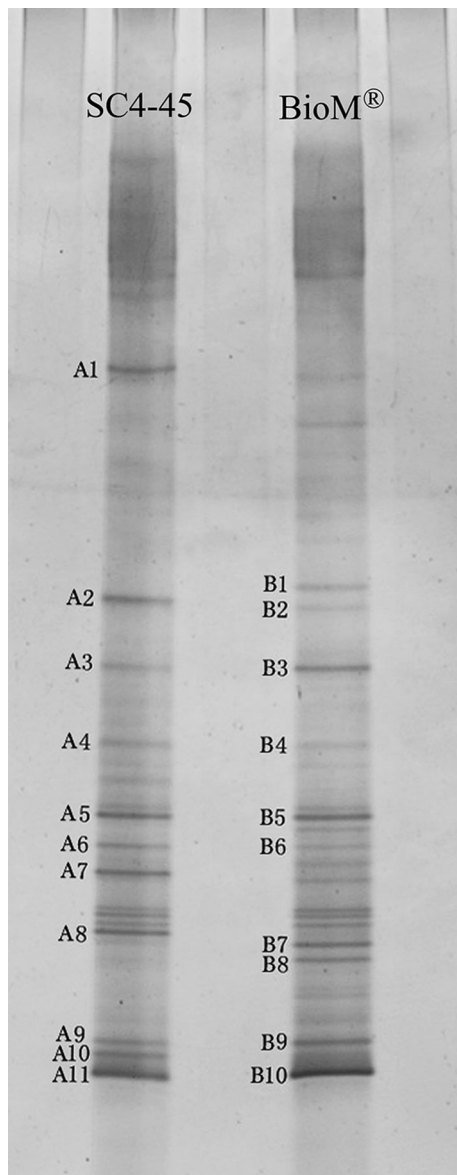


**Fig. 7** DGGE profiles of the biofilm samples obtained from SC4-45 and BioM<sup>®</sup> after 7 days of operation

similar, showed the value of 7.9–8.3, 7.6–8.0 and 7.7–8.2, respectively.

Figure 8a presents the COD removal efficiency of the MBBR reactors with different carriers under the start-up stage. The results indicated that bioreactor with SC4-45 had significant higher removal efficiency as compared to SC0 and BioM<sup>®</sup>. There was a slight difference between SC0 and BioM<sup>®</sup>. At the beginning, there was a sharp increase in the COD removal efficiency of SC4-45, reaching  $74.2 \pm 1.8$  % at day 2, and then it gradually rose with the time. The COD removal efficiency of SC4-45 at day 7 was  $99.5 \pm 1.1$  %, the effluent COD was less than 1.5 mg/L. Meanwhile, the removal efficiency of SC0 and

**Table 2** Closest relatives in the NCBI nucleotide sequence database based on 16S rRNA PCR-DGGE and gene sequences

| Band no. | Closest relative  | Similarity (%) | Accession no. |
|----------|---|----------------|---------------|
| A1       | <i>Sphaerotilus</i> sp. OT_B_418 16S ribosomal RNA gene                         | 98             | JQ945995.1    |
| A2       | <i>Tetrahymena capricornis</i> 16S ribosomal RNA gene                           | 100            | M98018.1      |
| A3       | <i>Aeromonas veronii</i> strain V_S_AN-4 16S ribosomal RNA gene                 | 96             | KJ186924.1    |
| A4       | <i>Bacterium</i> strain M233-4 partial 16S rRNA gene                            | 99             | HG792140.1    |
| A5       | <i>Flectobacillus</i> sp. Z13(2010) 16S ribosomal RNA gene                      | 100            | GU947862.1    |
| A6, B6   | <i>Aeromonas</i> sp. PR4_G10 partial 16S rRNA gene                              | 95             | HG932663.1    |
| A7       | Uncultured gamma proteobacterium clone ATB-LH-6394 16S ribosomal RNA gene       | 99             | FJ535220.1    |
| A8       | Uncultured <i>Pseudomonas</i> sp. clone LCB-10-77 16S ribosomal RNA gene        | 99             | KF692484.1    |
| A9, B9   | <i>Sphaerotilus natans</i> strain DSM 6575 16S ribosomal RNA gene               | 99             | NR_104787.1   |
| A10, B10 | <i>Sphaerotilus natans</i> strain NBRC 13543 16S rRNA gene                      | 98             | AB680432.1    |
| A11      | <i>Sphaerotilus</i> sp. BV-1 16S ribosomal RNA gene                             | 100            | JF824662.1    |
| B1       | Uncultured <i>Fluviicola</i> sp. clone cuticle_2.22 16S ribosomal RNA gene      | 99             | HQ111170.1    |
| B2       | <i>Tetrahymena sonneborni</i> strain EUR3d 18S small subunit ribosomal RNA gene | 100            | EF070258.1    |
| B3       | <i>Aeromonas schubertii</i> strain WL-1 16S ribosomal RNA gene                  | 96             | JQ303345.1    |
| B4       | Uncultured bacterium clone CEB2_8F_b04 16S ribosomal RNA gene                   | 98             | KC711485.1    |
| B5       | <i>Flectobacillus</i> sp. GFA-11 16S ribosomal RNA gene                         | 99             | EU420062.1    |
| B7       | <i>Flavobacterium lindanitolerans</i> strain Melo86 16S ribosomal RNA gene      | 97             | KC866179.1    |
| B8       | <i>Acidovorax</i> sp. CPO 4.0101 16S ribosomal RNA gene                         | 98             | KF923837.1    |

BioM<sup>®</sup> was almost 0 at day 2, and only  $67.0 \pm 2.1$  and  $74.9 \pm 2.7$  % after 7 days.

NH<sub>4</sub><sup>+</sup>-N removal efficiency is another important parameter in biological processes, which can also indicate the performance of the reactor. During the 7 days after

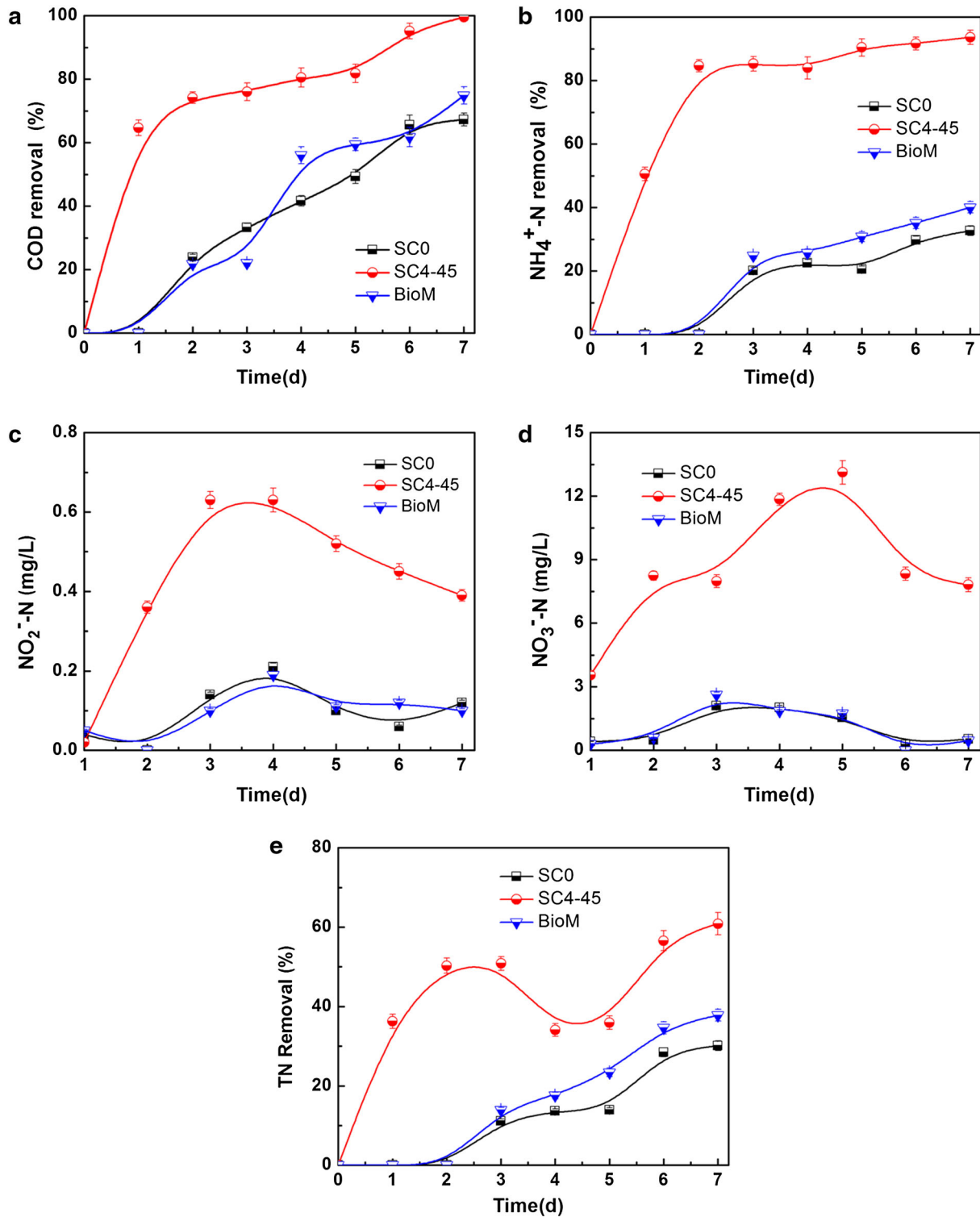


**Fig. 8** Wastewater treatment efficiency of SC4-45, SC0 and BioM<sup>®</sup> in the start-up stage (**a** COD removal efficiency, **b**  $\text{NH}_4^+\text{-N}$  removal efficiency, **c**  $\text{NO}_2^-\text{-N}$  concentration, **d**  $\text{NO}_3^-\text{-N}$  concentration, **e** TN removal efficiency)

seeding sludge,  $\text{NH}_4^+\text{-N}$  concentration decreased and  $\text{NH}_4^+\text{-N}$  removal efficiency increased with the time, as shown in Fig. 8b. Already  $84.7 \pm 2.2\%$  of  $\text{NH}_4^+\text{-N}$

removal efficiency was obtained for SC4-45 on day 2 and  $93.6 \pm 2.3\%$  on day 7, much higher than that of SC0 and BioM<sup>®</sup> on day 7,  $32.6 \pm 1.5\%$  and  $40.0 \pm 1.8\%$ ,

respectively. The effluent  $\text{NH}_4^+\text{-N}$  concentration kept stable at 1.6–3.9 mg/L in the following days meeting class A discharge standards, 5 mg/L (GB18918-2002, China). While  $\text{NH}_4^+\text{-N}$  removal efficiency were still lower than 40 % even on day 7, for SC0 and BioM<sup>®</sup>. As is well known, DO is high on the outside layer of the biofilm and aerobic nitrifiers, mainly nitrosomonas and nitriteoxidizer, oxidize ammonium-nitrogen ( $\text{NH}_4^+\text{-N}$ ) to oxidized nitrogen ( $\text{NO}_2^-\text{-N}$  and  $\text{NO}_3^-\text{-N}$ ). These autotrophic nitrifying bacteria grew slowly and were easily washed away, while they could be possibly the dominated population in biofilm due to the presence of the excellent attachment growth sites supplied by the porous structure. Hence, the home-made carriers with porous surface (SC4-45) had much higher nitrifying rate than SC0 and BioM<sup>®</sup> with smooth surface. Autotrophic nitrifying bacteria used  $\text{CO}_2$ ,  $\text{CO}_3^{2-}$ ,  $\text{HCO}_3^-$  as carbon sources. In the presence of  $\text{O}_2$ , the nitrosomonas oxidized ammonium to nitrites and nitriteoxidizer oxidized nitrites to nitrates. Thus,  $\text{NH}_4^+\text{-N}$  removal was achieved. It is obvious that the mass transfer of  $\text{NH}_4^+\text{-N}$  and  $\text{O}_2$  played a key role in this process. As mentioned above, SC4-45 had high attached biomass concentration and SC4-45 with proper thickness of biofilm had better mass transfer efficiency than SC2-45 and SC6-45. Therefore, SC4-45 exhibited the highest  $\text{NH}_4^+\text{-N}$  removal efficiency all the time, which is in accordance with the fact that SC4-45 has the highest  $\text{OUR}_{\text{NH}_4}$  of 17.4 mg  $\text{O}_2/\text{h}$ , about two times than others.

According to the practical operation and the literature, it can be regarded that the start-up was successful and the biofilm was stable when the removal efficiency of COD and  $\text{NH}_4^+\text{-N}$  exceeded 70 % [40]. Based on the above discussion, SC4-45 showed  $74.2 \pm 1.8$  % of COD removal efficiency and  $84.7 \pm 2.2$  % of  $\text{NH}_4^+\text{-N}$  removal efficiency on day 2. Moreover, the removal efficiencies were controlled at this level or even above this level until the end of the start-up. This indicates that SC4-45 has very quick start-up due to the special structure of the carrier and the optimal porous surface. On the contrarily, it takes 6 days for SC2-45 and SC6-45 to obtain the stable biofilm and the biofilm for SC0 and BioM<sup>®</sup> cannot reach stable even after 7 days.

During the 7 days after seeding sludge,  $\text{NO}_2^-\text{-N}$  concentration increased at first and then decreased with the time, as shown in Fig. 8c. It is clear that SC4-45 accumulated more  $\text{NO}_2^-\text{-N}$  than SC0 and BioM<sup>®</sup>. As mentioned above, the nitrosomonas oxidized ammonium to nitrites and nitrite oxidizer oxidized nitrites to nitrates. Hence, the concentration of  $\text{NO}_2^-\text{-N}$  was decided by the rates of nitrification and nitrosation [41]. For SC0 and BioM<sup>®</sup>, small quantities of  $\text{NH}_4^+\text{-N}$  was oxidized into  $\text{NO}_2^-\text{-N}$  by nitrification and  $\text{NO}_2^-\text{-N}$  could be transformed into  $\text{NO}_3^-\text{-N}$  fast by nitrosation because mass transfer is efficient in thin

biofilm. For SC4-45, the theoretical yield of  $\text{NO}_2^-\text{-N}$  should be the highest due to the fastest nitrification. However, the actual accumulated  $\text{NO}_2^-\text{-N}$  is low, because of the high attached biomass concentration and the high bacterial activity. It is important to notice that  $\text{NO}_2^-\text{-N}$  concentration in all the reactors was very low, even less than 0.75 mg/L.

During the 7 days after seeding sludge,  $\text{NO}_3^-\text{-N}$  concentration increased at first and then decreased with the time, as shown in Fig. 8d. It is clear that the home-made carriers accumulated  $\text{NO}_3^-\text{-N}$  as high as 14 mg/L, much more than SC0 and BioM<sup>®</sup>. For the home-made carriers, most of  $\text{NH}_4^+\text{-N}$  was oxidized into  $\text{NO}_2^-\text{-N}$  by nitrification and  $\text{NO}_2^-\text{-N}$  could be transformed into  $\text{NO}_3^-\text{-N}$  very easily by nitrosation; whereas, the  $\text{NO}_3^-\text{-N}$  removal is achieved by the process where anoxic heterotrophic denitrifiers reduced  $\text{NO}_3^-\text{-N}$  to  $\text{N}_2$  gas when DO decreases to a low level in the biofilm. In this process, denitrifiers needed to consume the readily biodegradable COD. The substrate mass transfer in the biofilm result in the slow denitrification and the  $\text{NO}_3^-\text{-N}$  accumulated in the reactor.

During the 7 days after seeding sludge, TN concentration increased at first and then fluctuated, as shown in Fig. 8e. SC4-45 achieved  $50.0 \pm 1.9$  % of TN removal efficiency on day 2,  $60.8 \pm 2.8$  % on day 7 and the average value of effluent TN was 14.9 mg/L. In view of small amount of suspended sludge in the MBBR, it is deduced that the TN was removed not only by assimilation into biomass, but also by simultaneous nitrification and denitrification (SND). Longer SRT could contribute to nitrification [42, 43], and Gong et al. [44] has achieved excellent performances of SND in biofilm processes by conducting complete SRT and SRT of  $42 \pm 4$  days. In our study, complete SRT was applied. Moreover, the novel carrier with large porosity surface avoided clogging effectively even under no wasted sludge discharge in MBBR. The SND process was caused by an oxygen diffusion limitation along the biofilm-inward depth. Porous microenvironment can be divided into two sub-microenvironments on the basis of DO gradient. DO concentration tends to decrease from periphery to the inside of the porous surface, providing oxic/aerobic zone at periphery for heterotrophs and nitrifiers and inner anoxic/anaerobic zone for denitrifiers. Hence, nitrification takes place at peripheral zones and denitrification in the deeper zones of the porous surface. This also was observed in a suspended carrier biofilm reactor by others [45, 46]. In the reactor based on SC4-45, over 80 %  $\text{NH}_4^+\text{-N}$  (influent concentration 25 mg/L) was removed as shown in Fig. 8b, while the highest concentration of  $\text{NO}_2^-\text{-N}$  in the reactor was only  $0.63 \pm 0.02$  mg/L and that of  $\text{NO}_3^-\text{-N}$  was only  $13.1 \pm 0.6$  mg/L as shown in Fig. 8c, d. The low concentration of nitrite confirms nitrite as the intermediate for a two-step nitrifications

scheme, and the first step is the rate limiting step. The rate of  $\text{NO}_3^-$ -N reduction (denitrification process) is slower than the rate of  $\text{NO}_3^-$ -N production (nitrification process). With the competition of denitrifier for substrate, mass transfer of electron acceptor and carbon source might be hindered inside the biofilm.

## Conclusions

A novel carrier with porous surface was firstly prepared by coating a sponge on the inside and outside of a hard polyethylene ring. The special structure is expected to be able to fasten the start-up of the reactor and enhance the mass transfer efficiency in the biofilm. The MBBRs based on the carriers were used to treat the synthetic wastewater (250 mg/L of COD and 25 mg/L of  $\text{NH}_4^+$ -N). The effects of the sponge thickness (0, 2, 4, 6 mm) and pore size (17, 45, 85 ppi) on the attached biomass concentration, and nutrient removal were investigated. The results showed that the optimal thickness of the porous layer was 4 mm and the optimal pore size was 45 ppi. After 7-day start-up, SC4-45 achieved higher overall bacterial activity compared to a commercial carrier BioM<sup>®</sup> and simple polyethylene rings (SC0), manifesting 17.4 mg  $\text{O}_2$ /h for  $\text{OUR}_{\text{NH}_4}$  and 150.1 mg  $\text{O}_2$ /h for  $\text{OUR}_{\text{COD}}$ . The DGGE fingerprints showed similar microbial population structure between SC4-45 and BioM<sup>®</sup> and 16S rRNA gene sequence analysis reveals dominance of *Sphaerotilus* sp. and *Aeromonas* sp. in biofilms of both carriers. For the MBBR based on SC4-45,  $74.2 \pm 1.8$  % of COD and  $84.7 \pm 2.2$  % of  $\text{NH}_4^+$ -N were removed on day 2 and they progressively increased to  $99.5 \pm 1.1$  and  $93.6 \pm 2.3$  %, respectively, until the end of the start-up, much better than BioM<sup>®</sup>. This indicated the novel carrier obtained a quick start-up.

**Acknowledgments** This research was supported by Nature Science Foundations of China (20977117, 21107146), Nature Foundations of Guangdong Province (92510027501000005), Science and Technology Research Programs of Guangzhou City (2012J4300118) and Project of Education Bureau of Guangdong Province (cgzhd1001), the Fundamental Research Funds for the Central Universities (121pgy20) and Innovative Talents Training Funding of Doctoral Students of Sun Yat-sen University and Scholarship Award for Excellent Doctoral Student Granted by Ministry of Education.

## References

- Daigger GT, Boltz JP (2011) Trickling filter and trickling filter-suspended growth process design and operation: a state-of-the-art review. *Water Environ Res* 83:388–404
- Zhou L, Zhang Z, Jiang W, Guo W, Ngo HH, Meng X, Fan J, Zhao J, Xia S (2008) Effects of low-concentration Cr (VI) on the performance and the membrane fouling of a submerged membrane bioreactor in the treatment of municipal wastewater. *Biofouling* 30(1):105–114
- Mixtli CP, Karim AA, Jesus Alberto MG, Marcela MT, Rolando TM, Luz MM, Marcelo V, Roberto PS (2012) Time and cost efficient biodegradation of diesel in a continuous-upflow packed bed biofilm reactor and effect of surfactant GAELE. *J Chem Technol Biotechnol* 87:1131–1140
- Filho JLRP, Sader LT, Damianovic MHRZ, Foresti E, Silva EL (2010) Performance evaluation of packing materials in the removal of hydrogen sulfide in gas-phase biofilters: polyurethane foam, sugarcane bagasse, and coconut fiber. *Chem Eng J* 158:441–450
- Pokhrel D, Hettiaratchi P, Patrick KS (2011) Methane diffusion coefficient in compost and soil-compost mixtures in gas phase biofilter. *Chem Eng J* 169:200–206
- Sevillano X, Isasi JR, Penas FJ (2012) Performance of a fluidized-bed bioreactor with hydrogel biomass carrier under extremely low-nitrogen availability and effect of nitrogen amendments. *J Chem Technol Biotechnol* 87:402–409
- Papadikis K, Gu S, Bridgwater AV (2010) A CFD approach on the effect of particle size on char entrainment in bubbling fluidized bed reactors. *Biomass Bioenerg* 34:21–29
- Hu XB, Xu K, Wang Z, Ding LL, Ren HQ (2013) Characteristics of biofilm attaching to carriers in moving bed biofilm reactor used to treat vitamin C wastewater. *Scanning* 35:283–291
- Tawfik A, El-Gohary F, Temmink H (2010) Treatment of domestic wastewater in an up-flow anaerobic sludge blanket reactor followed by moving bed biofilm reactor. *Bioprocess Biosyst Eng* 33:267–276
- Currie JA, Harrison NR, Wang L, Jones MI, Brooks MS (2007) A preliminary study of processing seafood shells for eutrophication control. *Asia Pac J Chem Eng* 2:460–467
- Gapes DJ, Keller J (2009) Impact of oxygen mass transfer on nitrification reactions in suspended carrier reactor biofilms. *Process Biochem* 44:43–53
- Aygun A, Nas B, Berkay A (2008) Influence of high organic loading rates on COD removal and sludge production in moving bed biofilm reactor. *Environ Eng Sci* 25:1311–1316
- Araujo MM Jr, Lermontov A, Araujo PL, Zaiat M (2013) Reduction of sludge generation by the addition of support material in a cyclic activated sludge system for municipal wastewater treatment. *Bioresour Technol* 143:483–489
- Tawfik A, Badr N, Abu Taleb E, El-Senousy W (2012) Sewage treatment in an up-flow anaerobic sponge reactor followed by moving bed biofilm reactor based on polyurethane carrier material. *Desalin Water Treat* 37:350–358
- Zhang S, Wang Y, He W, Wu M, Xing M, Yang J, Gao N, Pan M (2014) Impacts of temperature and nitrifying community on nitrification kinetics in a moving-bed biofilm reactor treating polluted raw water. *Chem Eng J* 236:242–250
- Zekker I, Rikmann E, Tenno T, Saluste A, Tomingas M, Menert A, Loorits L, Lemmiksoo V, Tenno T (2012) Achieving nitrification and anammox enrichment in a single moving-bed biofilm reactor treating reject water. *Environ Technol* 33:703–710
- Zekker I, Rikmann E, Tenno T, Lemmiksoo V, Menert A, Loorits L, Vabamäe P, Tomingas M, Tenno T (2012) Anammox enrichment from reject water on blank biofilm carriers and carriers containing nitrifying biomass: operation of two moving bed biofilm reactors (MBBR). *Biodegradation* 23:547–560
- Zekker I, Rikmann E, Tenno T, Vabamäe P, Kroon K, Loorits L, Saluste A, Tenno T (2012) Effect of  $\text{HCO}_3^-$  concentration on anammox nitrogen removal rate in a moving bed biofilm reactor. *Environ Technol* 33:2263–2271
- Nguyen TT, Ngo H, Guo W, Johnston A, Listowski A (2010) Effects of sponge size and type on the performance of an up-flow

- sponge bioreactor in primary treated sewage effluent treatment. *Bioresour Technol* 101:1416–1420
20. Garcia ML, Lapa KR, Foresti E, Zaiat M (2008) Effects of bed materials on the performance of an anaerobic sequencing batch biofilm reactor treating domestic sewage. *J Environ Manag* 88:1471–1477
  21. Valdivia A, Gonzalez-Martinez S, Wilderer PA (2007) Biological nitrogen removal with three different SBBR. *Water Sci Technol* 55:245–254
  22. Delatolla R, Berk D, Tufenkji N (2008) Rapid and reliable quantification of biofilm weight and nitrogen content of biofilm attached to polystyrene beads. *Water Res* 42:3082–3088
  23. Zekker I, Kroon K, Rikmann E, Tenno T, Tomingas M, Vabamäe P, Vlaeminck SE, Tenno T (2012) Accelerating effect of hydroxylamine and hydrazine on nitrogen removal rate in moving bed biofilm reactor. *Biodegradation* 23:739–749
  24. Bertin L, Lampis S, Todaro D, Scoma A, Vallini G, Marchetti L, Majone M, Fava F (2010) Anaerobic acidogenic digestion of olive mill wastewaters in biofilm reactors packed with ceramic filters or granular activated carbon. *Water Res* 44:4537–4549
  25. Hille A, He M, Ochmann C, Neu TR, Horn H (2009) Application of two component biodegradable carriers in a particle-fixed biofilm airlift suspension reactor: development and structure of biofilms. *Bioprocess Biosystems Eng* 32:31–39
  26. Odegaard H, Givsvold B, Strickland J (2000) The influence of carrier size and shape in the moving bed biofilm process. *Water Sci Technol* 41:383–391
  27. Cometti I, Gonzalez-Martinez S, Wilderer P (2004) Treatment of leachate from the anaerobic fermentation of solid wastes using two biofilm support media. *Water Sci Technol* 49:287–294
  28. Rasmussen K, Lewandowski Z (1998) Microelectrode measurements of local mass transport rates in heterogeneous biofilms. *Biotechnol Bioeng* 59:302–309
  29. Wei FS (2002) Monitoring and analysis method of water and wastewater. National Environmental Protection Agency, 4th edn. China Environmental Press, Beijing
  30. Chaiwat R, Tawan L, Benedict L, Eakalak K (2010) Relationship between respirometric activity and community of entrapped nitrifying bacteria: implications for partial nitrification. *Enzyme Microb Technol* 46:229–236
  31. Gorgensa JF, Van Zylb WH, Knoetze JH (2005) Reliability of methods for the determination of specific substrate consumption rates in batch culture. *Biochem Eng J* 25:109–112
  32. Tan C, Ma F, Qiu S (2013) Impact of carbon to nitrogen ratio on nitrogen removal at a low oxygen concentration in a sequencing batch biofilm reactor. *Water Sci Technol* 67:612–618
  33. Tay JH, Liu QS, Liu Y (2001) The effects of shear force on the formation, structure and metabolism of aerobic granules. *Appl Microbiol Biotechnol* 57:227–233
  34. Beer DD, Stoodley P, Lewandowski Z (1996) Liquid flow and mass transport in heterogeneous biofilms. *Water Res* 30: 2761–2765
  35. Awong J, Bitton G, Koopman B (1985) ATP oxygen uptake rate and INT-dehydrogenase activity of actinomycete foams. *Water Res* 19:917–921
  36. Nsabimana E, Belan A, Bohatier J (1999) Analysis at the genospecies level of microbial populations changes in activated sludge: the case of *Aeromonas*. *Water Res* 34:1696–1704
  37. Jassby D, Xiao Y, Schuler AJ (2014) Biomass density and filament length synergistically affect activated sludge settling: systematic quantification and modeling. *Water Res* 48(1):457–465
  38. Fu B, Liao X, Lian R, Ding L, Xu K, Ren H (2011) COD removal from expanded granular sludge bed effluent using a moving bed biofilm reactor and their microbial community analysis. *World J Microbiol Biotechnol* 27:915–923
  39. Chen Q, Qu L, Tong G, Ni J (2011) Simultaneous nutrients and carbon removal from low-strength domestic wastewater with an immobilized microorganism biological aerated filter. *Water Sci Technol* 63:885–890
  40. Jiang F (2006) Biological properties of material and structure of suspended bio-carriers and cage-type bioreactor. Dissertation for Ph.D. South China University of Technology
  41. Qiao XL, Chen QX, Zhang ZJ (2008) Comparative study of nitrification performances of immobilized cell fluidized bed reactor and contact oxidation biofilm reactor in treating high strength ammonia wastewater. *J Chem Technol Biotechnol* 83:84–90
  42. Rahimi Y, Torabian A, Mehrdadi N, Shahmoradi B (2011) Simultaneous nitrification–denitrification and phosphorus removal in a fixed bed sequencing batch reactor (FBSBR). *J Hazard Mater* 185:852–857
  43. Walters E, Hille A, He M, Ochmann C, Horn H (2009) Simultaneous nitrification/denitrification in a biofilm airlift suspension (BAS) reactor with biodegradable carrier material. *Water Res* 43:4461–4468
  44. Gong L, Jun L, Yang Q, Wang S, Ma B, Peng Y (2012) Biomass characteristics and simultaneous nitrification–denitrification under long sludge retention time in an integrated reactor treating rural domestic sewage. *Bioresour Technol* 119:277–284
  45. Yang S, Yang F, Fu Z, Lei R (2009) Comparison between a moving bed membrane bioreactor and a conventional membrane bioreactor on organic carbon and nitrogen removal. *Bioresour Technol* 100:2369–2374
  46. Khan SJ, Ilyas S, Javid S, Visvanathan C, Jegatheesan V (2011) Performance of suspended and attached growth MBR systems in treating high strength synthetic wastewater. *Bioresour Technol* 102:5331–5336